Optics EXPRESS

High speed time-of-flight displacement measurement based on dual-comb electronically controlled optical sampling

YIYI SHI, DINGTONG HU, RUI XUE, ZILING WU, JIAQI DONG, HAOCHEN TIAN, CHUNZE WANG, JIAQI WANG, MINGLIE HU, AND YOUJIAN SONG*

Ultrafast Laser Laboratory, Key Laboratory of Opto-electronic Information Science and Technology of Ministry of Education, School of Precision Instruments and Opto-electronics Engineering, Tianjin University, Tianjin 300072, China

*yjsong@tju.edu.cn

Abstract: We demonstrate a direct time-of-flight approach that utilizes dual-comb electronically controlled optical sampling (ECOPS) to measure small displacements. ECOPS is enabled by electrically controlling the repetition rate of one laser via an intracavity electric-optical modulator (EOM). The acquisition rate is set by the EOM modulation frequency, which is much higher than commonly used asynchronous optical sampling (ASOPS). In a proof-of-principle experiment, an 80-kHz acquisition rate is obtained with a pair of ~105 MHz repetition rate Er-fiber lasers. At an average time of 30 ms, a measurement precision evaluated with Allan deviation reaches 26.1 nm for a 40-µm static displacement. In a dynamic measurement, a 500-Hz sinusoidal vibration with 15 µm amplitude has also been identified. The high-precision and high-speed displacement measurement technique can be potentially used in 3D surface profilometry of microelectronic step-structures and real-time monitoring of high frequency mechanical vibrations, etc.

1. Introduction

Femtosecond laser optical frequency comb [1,2] has become an enabling technology in many fields, such as optical atomic clock [3], precision metrology [4,5], molecular spectroscopy [6], microwave photonics [7], etc. In particular, a dual-comb scheme [8–17] has been intensively studied for applications in length metrology [9–12], Fourier transform spectroscopy [13–15], time and frequency transfer [16,17]. The dual-comb scheme is based on two synchronized femtosecond lasers with a slight offset repetition rate. The pulse sequences of the two lasers continuously walk off from each other in time domain, resulting in asynchronous optical sampling (ASOPS) process [18]. ASOPS has been frequently used for time-of-flight (TOF) ranging [9–12], where the exact timing between the returning reference and target pulses can be determined in an effective coordinate with temporal magnification.

The acquisition rate of ASOPS-based TOF ranging is determined by the repetition rate difference between the two combs. For commonly used ~100-MHz repetition-rate mode-locked fiber lasers, the acquisition rate is limited to several kHz for adequate sampling. Alternative to ASOPS, attempts have been made to adjust the scan range and scan speed by electronically controlling the relative time delay of two laser pulse sequences. The so called electronically controlled optical sampling (ECOPS) technology [19–24] is currently widely used as fast delay lines in Terahertz time-domain spectroscopy (THz-TDS) systems [20–23]. Recently, dual-comb coherent anti-Stokes Raman scattering (DC-CARS) spectroscopy employing ECOPS method is also presented [24]. In contrast to conventional DC-CARS spectroscopy, ECOPS shows a record-high spectral acquisition rate of 100000 spectra/s and higher sensitivity.

#454981
Journal © 2022

https://doi.org/10.1364/OE.454981
Received 2 Feb 2022; accepted 17 Feb 2022; published 25 Feb 2022

Optics EXPRESS

Different from ASOPS scheme which scans the entire repetition period of the pulse train, the ECOPS scheme allows to selectively scan a small portion of the repetition period which exactly covers the returning reference and target pulses. This is particularly useful for small displacement measurement and the acquisition rate can be significantly increased. In this paper, we show that ECOPS scheme provides a route to TOF measurement with high speed. We use two nonlinear polarization evolution (NPE) mode-locked Er-fiber lasers with 105 MHz repetition rate to demonstrate displacement measurement based on ECOPS. The two lasers are tightly synchronized by the balanced optical cross-correlation (BOC) technique [25–27]. Then, a square wave modulation has been applied to a high-bandwidth electro-optic phase modulator (EOM) inside one laser, thus enables ECOPS. The sampled signals are collected via two-photon absorption process in an avalanched photodetector (APD) and the TOF is calculated in computer after data collection. In a proof-of-principle experiment, we characterized a static small-range displacement and a vibrational object. The acquisition rate is as high as 80 kHz. In the static measurement of a 40-μm displacement, the Allen deviation reaches 26.1 nm at an averaging time of 30 ms. In the dynamic measurement, the trajectory of a sinusoidal vibrational piezo actuator with a frequency of 500 Hz and an amplitude of 15 μm has been obtained.

2. Principle

Figure 1 illustrates the principle of ECOPS-based TOF measurement technology. A pair of lasers with equal repetition rate f_{rep} is used for TOF measurement. The pulses from signal laser are directed to reference and target, and the echo pulse sequences are sampled by local oscillator. An EOM is used to periodically switch the repetition rate of local oscillator from $f_{rep} + \Delta f$ to $f_{rep} - \Delta f$, with the modulation frequency of f_{mod}. During each half of modulation period, the temporal delay Δt between the reference and the target can be precisely characterized in a stretched timescale. The acquisition rate is as high as $2f_{mod}$, limited by modulation bandwidth of EOM.

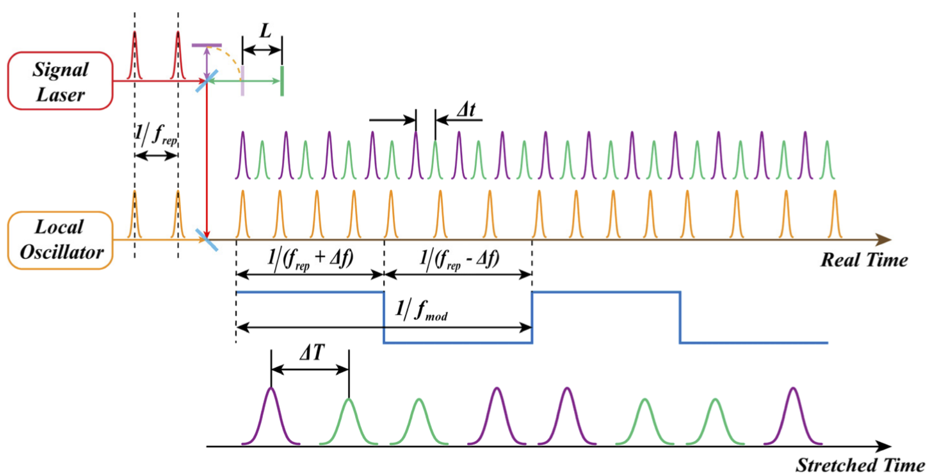

Fig. 1. Time-domain schematic of ECOPS-based TOF measurement technology. The repetition rate of local oscillator is switched between $f_{rep} + \Delta f$ and $f_{rep} - \Delta f$. The frequency of square wave modulation is f_{mod} and the acquisition rate is equal to $2f_{mod}$.

The distance L between the target and the reference is

$$L = \frac{c\Delta T}{2n_g}\frac{\Delta f}{f_{rep}}, \tag{1}$$

where c is the speed of light in vacuum, n_g is the group refractive index in air, ΔT is the obtained TOF in the stretched timescale. Before calculating L, the value of Δf should be determined in advance. The repetition rate difference Δf is related with the single walk-off distance ($\Delta d_{walk-off}$) between the sampling pulse and the measuring pulse as

$$\Delta d_{walk-off} = \left|\frac{1}{f_{rep}} - \frac{1}{f_{rep} \pm \Delta f}\right| \times \upsilon_g \approx \frac{\Delta f}{f_{rep}^2}\upsilon_g, \tag{2}$$

where υ_g is the group velocity of pulses in air. Given that $\Delta d_{walk-off} = \Delta D/n_g$, where ΔD is the optical path variation introduced by electro-optic modulation inside local oscillator, consequently,

$$\Delta f = \frac{\Delta D}{n_g}\frac{f_{rep}^2}{\upsilon_g} = \frac{f_{rep}^2 \Delta D}{c}. \tag{3}$$

ΔD can be determined according to the electro-optic phase delay:$\varphi = \pi V/V_\pi$, where V is the voltage applied to EOM, V_π is the half-wave voltage of electro-optic crystal, thus $\Delta D = (\varphi/\pi)\lambda/2 = \lambda V/(2V_\pi)$. Therefore, Eq. (3) can be expressed as

$$\Delta f = \frac{\lambda f_{rep}^2 V}{2cV_\pi}. \tag{4}$$

Equation (1) is finally expressed as

$$L = \frac{\lambda f_{rep} \Delta T V}{4n_g V_\pi}. \tag{5}$$

There is a maximum measurable distance L_{max} determined by accumulated walk-off distance between sampling pulses and measuring pulses during each half of square wave modulation period of $1/2f_{mod}$. Given the number of pulses undergoing walk off is $1/2f_{mod}/(1/f_{rep}) = f_{rep}/2f_{mod}$, the maximum measurable distance L_{max} can be represented by

$$L_{max} = \Delta d_{walk-off} \times \frac{f_{rep}}{2f_{mod}} = \frac{\lambda f_{rep} V}{4n_g f_{mod} V_\pi}. \tag{6}$$

Our system employs lasers with a repetition rate of 105 MHz and a wavelength of 1.5 µm, and the modulation frequency is set to 80 kHz. The half-wave voltage of EOM is 350 V, and the maximum voltage applied to EOM reaches 200 V owing to the limited experimental conditions. Consequently, the calculated L_{max} is about 280 µm.

3. Experimental setup

The displacement measurement configuration based on ECOPS is shown in Fig. 2(a). We utilized a pair of NPE mode-locked lasers [28,29] operating at repetition rates of ∼ 105 MHz. Laser 1 (Fig. 2(b)) serves as local oscillator (LO), while laser 2 (Fig. 2(c)) is signal laser. An EOM is inserted into Laser 1 to periodically modulate repetition rate. Since the EOM requires a vertically polarized incoming laser beam, a half wave plate is placed before the EOM to align the polarization state. Laser 2 contains a segment of linear optical path, where the end mirror is glued to a piezo actuator (PZT) for repetition-rate locking. Both lasers are output from a polarization beam-splitter (PBS).

The synchronization of two pulse sequences is achieved by the balanced optical cross-correlation module (BOC) technique. A single crystal balanced optical cross-correlator is used to detect the relative timing error and to convert it into error voltage. Then, the error voltage is sent to a PI servo controller (New Focus, LB1005), whose output voltage is amplified and fed back

Optics EXPRESS

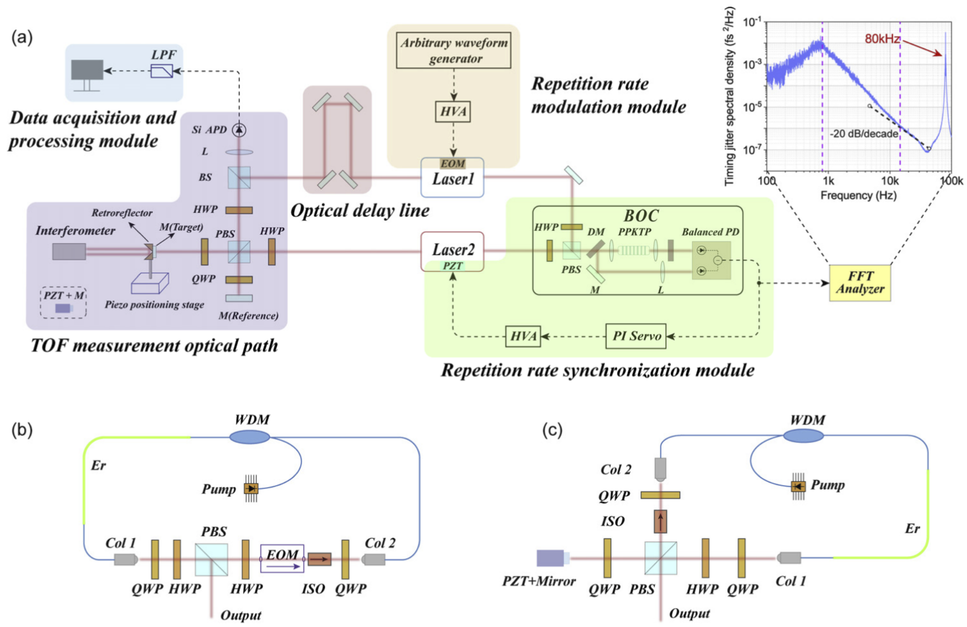

Fig. 2. Demonstration of displacement measurement system. (a) Experimental setup. The inset shows the timing jitter spectrum of the synchronization system. (b) and (c) The configuration of two NPE mode-locked lasers. PZT: piezo actuator; EOM: electro-optic modulator; BOC: balanced optical cross-correlation; HWP: half-wave plate; PBS: polarization beam splitter; DM: dichroic mirror; M: mirror; L: lens; PPKTP: periodically poled KTP; Balanced PD: balanced photodetector; PI Servo: proportional-integral servo controller; HVA: high voltage amplifier; QWP: quarter wave plate; BS: beam splitter; Si APD: silicon avalanche photodetector; LPF: low pass filter. WDM: wavelength division multiplexer; Er: erbium-doped gain fiber; Col: collimator; ISO: isolator.

to the PZT in the laser 2, thus close the phase-locked loop. The two temporally synchronized pulse sequences are sent to the TOF measurement optical path, as illustrated in Fig. 2(a). The pulse train from Laser 2 is directed to target and reference mirrors, and the returning pulses are combined with pulse train from Laser 1. An optical delay line is used to temporally align pulses from Laser 1 to the returning target and reference pulses.

ECOPS is achieved by modulating intracavity EOM in Laser 1. An arbitrary waveform generator generates a square wave with a duty cycle of 50% and a frequency of 80 kHz. The modulation signal is voltage amplified and applied to the EOM, so as to periodically modulate the refractive index of the extraordinary axis of electro-optic crystal. The repetition rate phase-locking based on BOC method has been established in the presence of EOM modulation. The PI corner has been set as 1 kHz. The inset in Fig. 2(a) shows the in-loop residual timing jitter spectrum measured with an FFT analyzer (Stanford Research Systems, SR770) after lock-on. The power spectrum shows that the locking bandwidth is about 800 Hz. An 80 kHz modulation frequency is also clearly visible in the spectrum. Below 800 Hz, the pulse trains from the two lasers are temporally synchronized. Above 800 Hz, the curve rolls off until a −20 dB/decade slope is observed at 15 kHz offset frequency. This is a signature of random walk and reflects a quantum noise limited timing jitter between the two lasers [30,31], meaning that impact of servo control vanishes above 15 kHz. Therefore, cross-talk between the EOM modulation and synchronization system is avoided effectively. Consequently, Laser 1 scans the repetitive returning pulse pairs from target and reference mirrors, and the cross-correlation trace is photo-detected for TOF extraction.

Optics EXPRESS

In this experiment, a nonlinear sampling technique based on two-photon absorption (TPA) effect [32] has been used to generate stable cross-correlation signals. To this end, two pulse sequences are simply beam-combined and focused to a Silicon APD by a lens. Each cross-correlation signal is low-pass filtered to extract the envelop from the interferometric cross-correlation traces. The filtered signals are collected by a digitizer (National Instruments, PXIe-5122). The subsequent data processing and distance calculation procedures are conducted in computer.

4. Experimental results

The cross-correlation signals obtained by applying an 80-kHz square wave modulation signal to Laser 1 after establishing the repetition rate synchronization is shown in Fig. 3(a). The pulses with lower intensity are target signals, and the pulses with higher intensity are reference signals. The period of down-sampled signals in the Fig. 3(a) is about 12.5 µs, which exactly corresponds to the modulation period (Fig. 3(b)). In each period, there are two sets of down-sampled signals, marked as yellow background and blank. They represent for two halves of a modulation period, respectively. It can be seen from Fig. 3(c) that two pulses both have pedestals on the left side, which is caused by the pedestal in output pulses of laser 1. It should be noted that these pedestals won't affect the extraction of the peak positions of pulses.

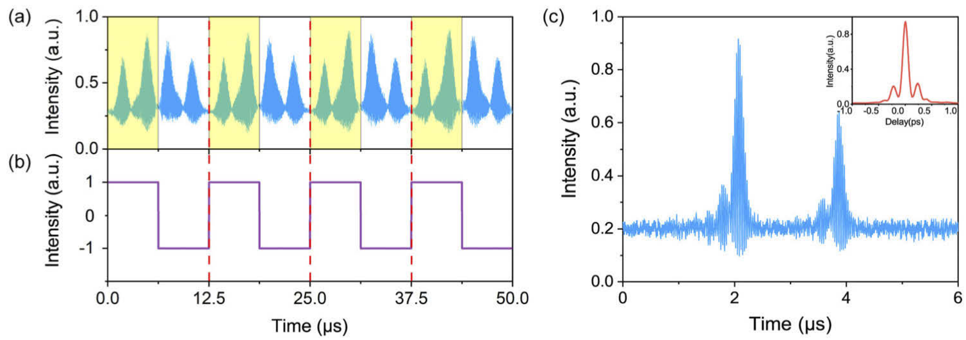

Fig. 3. The cross-correlation signals and modulation signal. (a) Part of the cross-correlation signals when the frequency of square wave is 80kHz. (b) Modulation signal. (c) One cross-correlation trace after low pass filtering. The inset shows the autocorrelation trace of pulse from laser 1.

To test the accuracy of dual-comb displacement measurement system, a comparison experiment using a commercial laser interferometer (Renishaw, XL-80) was conducted. The laser interferometer has a linear measurement precision of ±0.5 ppm and a linear resolution of 1 nm. In the TOF measurement optical path of Fig. 2(a), a half-inch silver mirror is glued to back of the retroreflector and they are fixed on a piezo positioning stage together. The silver mirror is the target of displacement measurement system, and the retroreflector is the target mirror of interferometer. The measurement results of 5 positions during the range of 0–40 µm are illustrated in Fig. 4(a). Each measured displacement is an averaged result with 2000 average times. It can be seen from the blue curve of Fig. 4(a) that there is a good linear relationship between results of this system and interferometer. In the orange curve of Fig. 4(a), the maximum residual between the measured value and the interferometer reference value does not exceed 0.4 µm, and the maximum standard deviation of the measured value is about 50 nm. The precision is evaluated by Allan deviation, as shown in Fig. 4(b), reaching ∼26.1 nm with 30 ms averaging time.

This system is also suitable for measuring small-amplitude vibrations. We replace the target with a small mirror glued on a piezo actuator (as shown in the black dashed box in the purple

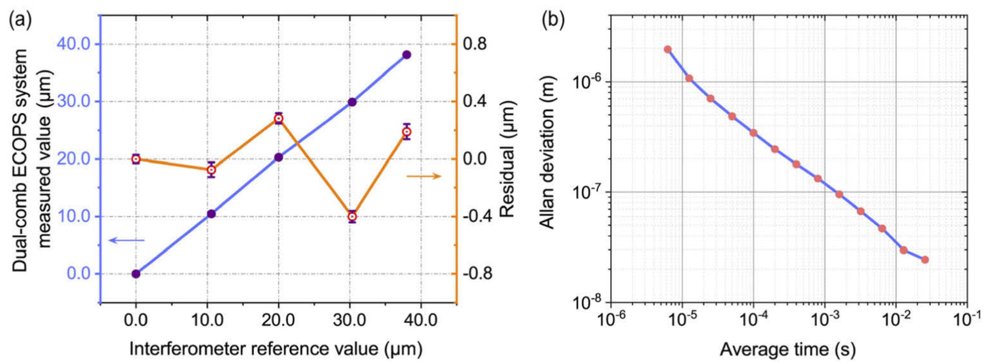

Fig. 4. The displacement measurement results. (a) Experimental results with 30 ms averaging time in comparison with the data obtained by the interferometer. (b) The Allan deviation at a fixed measurement displacement of 30 μm.

area of Fig. 2(a)). We apply a 50 V sinusoidal voltage with a frequency of 500 Hz to PZT. The calculated unloaded vibration amplitude is ∼15 μm. The vibration test result is shown in Fig. 5. There are 50 sine periods in total (Fig. 5(a)), and 10 sine periods are intercepted and amplified (Fig. 5(b)). The period of sinusoidal wave is 2 ms, which is consistent with the applied vibration frequency. The vibration range is about 12 μm, slightly less than the calculation because PZT carries a mirror. In addition, we perform Fourier transform analysis on the vibration test result of Fig. 5(a) to obtain its frequency components, as shown in Fig. 5(c). The strongest frequency component is 500 Hz, which is exactly the target vibration frequency we applied. Some very low-intensity noise harmonic signals are also found. Theoretically, the acquisition rate can reach $2f_{mod}$(i.e. 160 kHz). Nevertheless, in the actual vibration test experiment, we utilize one pulse pair in each modulation period to calculate target distance. Therefore, the actual acquisition rate is 80 kHz.

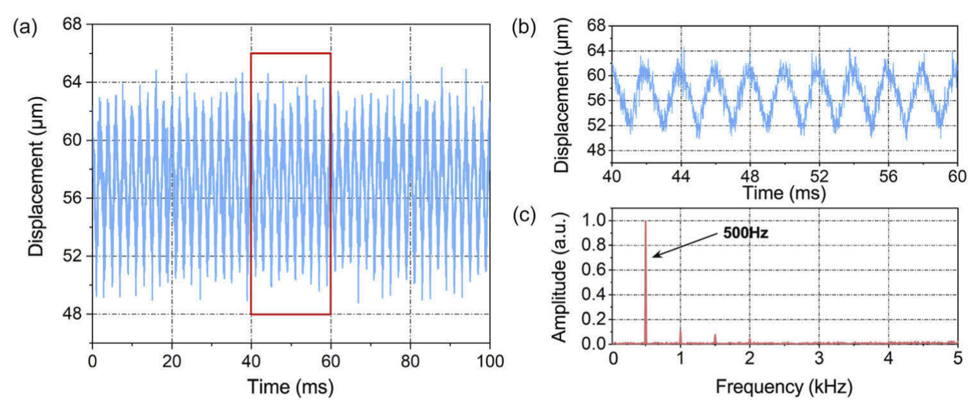

Fig. 5. Experimental results of small-amplitude vibration when the acquisition rate is 80 kHz. (a) and (b) 500 Hz sinusoidal vibration with 12 μm amplitude. (c) Fourier analysis of vibration test result.

5. Conclusion

In conclusion, a dual-comb time-of-flight displacement measurement method with high acquisition rate was presented in this paper. Based on two NPE mode-locked fiber lasers, we achieved

Optics EXPRESS

electronically controlled optical sampling through intracavity electro-optic phase modulator. We verified the accuracy and precision of displacement measurement system by using a commercial laser interferometer, and the static experimental results revealed that the precision can reach ~26.1 nm with 30 ms averaging time. Then we tested the sinusoidal vibration with a frequency of 500 Hz and an amplitude of 15 μm of PZT. The vibration test results indicated the capacity of this system for measuring small amplitude vibrations. Compared with the traditional dual-comb ASOPS time-of-flight ranging method utilizing the same repetition rate fiber lasers, the acquisition rate is increased by ~ 40 times.

The price for maintaining high acquisition rate is the limited maximum measurable distance L_{max}. Therefore, our system is more suitable for measuring small displacements or fast vibrations with small amplitude. According to Eq. (6), expanding the maximum measurable distance needs higher f_{rep}, which can be achieved by using higher repetition-rate sources (i.e. micro-resonator combs). Furthermore, raising V/V_{π} ratio can also increase L_{max}. Using the waveguide-type electro-optic modulator with a smaller half-wave voltage may multiply the V/V_{π} ratio more conveniently.

It is also interesting to compare this work with a recent direct TOF displacement measurement experiment by Y. Na, et al. [5]. By utilizing an electro-optic-sampling-based timing detector (EOS-TD), a TOF displacement measurement with sub-nanometer precision and nanosecond acquisition time has been demonstrated. Y. Na's approach is advantageous of high precision, ultrafast speed and only one mode-locked laser is required. Being distinct from EOS-TD, the ECOPS-based configuration demonstrated here is compatible with interferometric measurements as well as powerful dual-comb spectroscopy by further referencing one comb line to a CW laser. To this end, a fringe-counting based interferometric measurement may enable sub-nanosecond precision comparable with [5]. On the other hand, the Fourier transform of the interferometric pattern naturally presents comb-line resolved absorptive spectrum. The combined function of displacement measurement and spectroscopy may provide a novel optical diagnostic tool and allow hyperspectral-imaging with high optical resolution.

Funding. National Natural Science Foundation of China (61827821, 61975144).

Acknowledgments. We thank Prof. Jianqiang Gu for fruitful discussions.

Disclosures. The authors declare no conflicts of interest.

Data availability. Data underlying the results presented in this paper are not publicly available at this time but may be obtained from the authors upon reasonable request.

References

1. S. T. Cundiff and J. Ye, "Colloquium: Femtosecond optical frequency combs," Rev. Mod. Phys. **75**(1), 325–342 (2003).
2. J. L. Hall, "Nobel Lecture: Defining and measuring optical frequencies," Rev. Mod. Phys. **78**(4), 1279–1295 (2006).
3. N. Nemitz, T. Ohkubo, M. Takamoto, I. Ushijima, M. Das, N. Ohmae, and H. Katori, "Frequency ratio of Yb and Sr clocks with $5\times10{-}17$ uncertainty at 150 seconds averaging time," Nat. Photonics **10**(4), 258–261 (2016).
4. K. Minoshima and H. Matsumoto, "High-accuracy measurement of 240-m distance in an optical tunnel by use of a compact femtosecond laser," Appl. Opt. **39**(30), 5512–5517 (2000).
5. Y. Na, C.-G. Jeon, C. Ahn, M. Hyun, D. Kwon, J. Shin, and J. Kim, "Ultrafast, sub-nanometre-precision and multifunctional time-of-flight detection," Nat. Photonics **14**(6), 355–360 (2020).
6. S. A. Diddams, L. Hollberg, and V. Mbele, "Molecular fingerprinting with the resolved modes of a femtosecond laser frequency comb," Nature **445**(7128), 627–630 (2007).
7. T. M. Fortier, M. S. Kirchner, F. Quinlan, J. Taylor, J. C. Bergquist, T. Rosenband, N. Lemke, A. Ludlow, Y. Jiang, C. W. Oates, and S. A. Diddams, "Generation of ultrastable microwaves via optical frequency division," Nat. Photonics **5**(7), 425–429 (2011).
8. R. Liao, H. Tian, W. Liu, R. Li, Y. Song, and M. Hu, "Dual-comb generation from a single laser source: Principles and spectroscopic applications towards mid-IR-A review," J. Phys. Photonics **2**(4), 042006 (2020).
9. I. Coddington, W. C. Swann, L. Nenadovic, and N. R. Newbury, "Rapid and precise absolute distance measurements at long range," Nat. Photonics **3**(6), 351–356 (2009).
10. R. Jiang, S. Zhou, and G. Wu, "Aliasing-free dual-comb ranging system based on free-running fiber lasers," Opt. Express **29**(21), 33527–33535 (2021).

Optics EXPRESS

11. T. Mitchell, J. Sun, and D. T. Reid, "Dynamic measurements at up to 130-kHz sampling rates using Ti:sapphire dual-comb distance metrology," Opt. Express **29**(25), 42119–42126 (2021).
12. H. Shi, Y. Song, R. Li, Y. Li, H. Cao, H. Tian, B. Liu, L. Chai, and M. Hu, "Review of low timing jitter mode-locked fiber lasers and applications in dual-comb absolute distance measurement," Nanotechnol. Precis. Eng. **1**(4), 205–217 (2018).
13. I. Coddington, W. C. Swann, and N. R. Newbury, "Coherent multiheterodyne spectroscopy using stabilized optical frequency combs," Phys. Rev. Lett. **100**(1), 013902 (2008).
14. S. Boudreau and J. Genest, "Referenced passive spectroscopy using dual frequency combs," Opt. Express **20**(7), 7375–7387 (2012).
15. I. Coddington, N. Newbury, and W. Swann, "Dual-comb spectroscopy," Optica **3**(4), 414–426 (2016).
16. F. R. Giorgetta, W. C. Swann, L. C. Sinclair, E. Baumann, I. Coddington, and N. R. Newbury, "Optical two-way time and frequency transfer over free space," Nat. Photonics **7**(6), 434–438 (2013).
17. H. Lu, Z. Li, J. Wang, H. Meng, and J. Zhao, "Two-way optical time and frequency transfer over a 20-km fiber link based on optical frequency combs," IEEE Photonics J. **11**(1), 1–7 (2019).
18. R. Gebs, G. Klatt, C. Janke, T. Dekorsy, and A. Bartels, "High-speed asynchronous optical sampling with sub-50fs time resolution," Opt. Express **18**(6), 5974–5983 (2010).
19. F. Tauser, C. Rausch, J. H. Posthumus, and F. Lison, "Electronically controlled optical sampling using 100 MHz repetition rate fiber lasers," Proc. SPIE **6881**, 68810O (2008).
20. Y. Kim and D.-S. Yee, "High-speed terahertz time-domain spectroscopy based on electronically controlled optical sampling," Opt. Lett. **35**(22), 3715–3717 (2010).
21. M. Oeri, O. Peters, M. Wolferstetter, and R. Holzwarth, "Compact, high-speed sampling engine for pulsed femtosecond lasers," Proc. SPIE **11348**, 8 (2020).
22. R. J. B. Dietz, N. Vieweg, T. Puppe, A. Zach, B. Globisch, T. Göbel, P. Leisching, and M. Schell, "All fiber-coupled THz-TDS system with kHz measurement rate based on electronically controlled optical sampling," Opt. Lett. **39**(22), 6482–6485 (2014).
23. M. Yahyapour, A. Jahn, K. Dutzi, T. Puppe, P. Leisching, B. Schmauss, N. Vieweg, and A. Deninger, "Fastest thickness measurements with a Terahertz time-domain system based on electronically controlled optical sampling," Appl. Sci. **9**(7), 1283 (2019).
24. R. Kameyama, S. Takizawa, K. Hiramatsu, and K. Goda, "Dual-comb coherent Raman spectroscopy with near 100% duty cycle," ACS Photonics **8**(4), 975–981 (2021).
25. T. R. Schibli, J. Kim, O. Kuzucu, J. T. Gopinath, S. N. Tandon, G. S. Petrich, L. A. Kolodziejski, J. G. Fujimoto, E. P. Ippen, and F. X. Kaertner, "Attosecond active synchronization of passively mode locked lasers by balanced cross correlation," Opt. Lett. **28**(11), 947–949 (2003).
26. J. Kim, J. Chen, Z. Zhang, F. N. C. Wong, F. X. Kärtner, F. Loehl, and H. Schlarb, "Long-term femtosecond timing link stabilization using a single crystal balanced cross correlator," Opt. Lett. **32**(9), 1044–1046 (2007).
27. H. Tian, N. Raabe, Y. Song, G. Steinmeyer, and M. Hu, "High-detectivity optical heterodyne method for wideband carrier-envelope phase noise analysis of laser oscillators," Opt. Lett. **43**(13), 3108–3111 (2018).
28. V. J. Matsas, D. J. Richardson, T. P. Newson, and D. N. Payne, "Characterization of a self-starting, passively mode-locked fiber ring laser that exploits nonlinear polarization evolution," Opt. Lett. **18**(5), 358–360 (1993).
29. A. Komarov, H. Leblond, and F. Sanchez, "Theoretical analysis of the operating regime of passively-mode-locked fiber laser through nonlinear polarization rotation," Phys. Rev. A **72**(6), 063811 (2005).
30. H. A. Haus and A. Mecozzi, "Noise of mode-locked lasers," IEEE J. Quantum Electron. **29**(3), 983–996 (1993).
31. J. Kim and Y. Song, "Ultralow-noise mode-locked fiber lasers and frequency combs: principles, status, and applications," Adv. Opt. Photonics **8**(3), 465–540 (2016).
32. J. A. Giordmaine, P. M. Rentzepis, S. L. Sham, and K. W. Wecht, "Two-photon excitation of fluorescence by picosecond light pulses," Appl. Phys. Lett. **11**(7), 216–218 (1967).